# QUASI-EULERIAN FORMULATION FOR FLUID-STRUCTURE INTERACTION

by

J. M. Kennedy, T. Belytschko and D. F. Schoeberle

Prepared for

5th SMiRT Conference

Berlin, Germany

August 13-17, 1979

U of C-AUA-USDOE

ARGONNE NATIONAL LABORATORY, ARGONNE, ILLINOIS

Operated under Contract W-31-109-Eng-38 for the

U. S. DEPARTMENT OF ENERGY

Summary

Fluid-structure interaction problems become particularly difficult to [illegible] are large. Eulerian descriptions for the fluid are not well suited to [illegible] cause the structure must be described by a Lagrangian mesh, so that considerable [illegible] difficulties are entailed in treating the motion of the Lagrangian mesh [illegible] fixed fluid mesh. Lagrangian descriptions for the fluid, although [illegible] with Lagrangian meshes for the structure, become very distorted if the time [illegible] is sufficiently large. For these reasons, numerous investigators have taken recourse to what are often called arbitrary Lagrangian-Eulerian formulations or quasi-Eulerian formulations in which the fluid mesh nodes can move in space independently of the material; this permits the fluid nodes which are in contact with the structure to be moved with the structure in the direction normal so that the difficulties inherent in Eulerian formulations are avoided. Most available formulations of this type are however in a finite difference format, which limits their usefulness in engineering applications.

In this paper, recent developments of a quasi-Eulerian finite element formulation for the treatment of the fluid in fluid-structure interaction problems are described. The present formulation is applicable both to plane two-dimensional and axisymmetric three-dimensional problems. In order to reduce the noise associated with the convection terms, an amplification factor technique is used to implement an up-winding type scheme.

The application of the method is illustrated in two problems which are of importance in nuclear reactor safety:

1. A two-dimensional model of a cross section of a subassembly configuration, where the quasi-Eulerian formulation is used to model the fluid adjacent to the structures and in the channel between the subassemblies.

2. Pressure transients in a straight pipe, where the axisymmetric formulation is used to model the fluid in the pipe.

These results are compared to experimental results for these problems and compare quite well.

The major problem in the application of these methods appears to be the automation of the scheme for moving the fluid nodes. Several alternative schemes are used in the problems described here, and a more general scheme which appears to offer a reasonable compromise between versatility and ease of use is described.

## 1. Introduction

The advantages of Quasi-Eulerian formulations for modelling fluids in fluid-structure interaction analysis with large displacements is readily apparent. Lagrangian formulations for the fluid, when used in these analysis, suffer from severe distortions of the mesh, which must be corrected by rezoning several times during the computation. These rezoning procedures add considerable expense to a computation; usually the analyst stops the computation, designs a rezone and then proceeds to compute the next series of time steps. In today's computer environment, large analyses are generally still done overnight, so that a fluid-structure interaction analysis performed with rezones often stretches over one or two weeks of real time. Furthermore, rezones introduce errors into momentum and energy balance. Even with rezones, a Lagrangian procedure cannot satisfactorily treat flow around corners. Considerable progress has lately been made in "continuous rezoning procedures" in which small alterations are made in a Lagrangian mesh to minimize distortion; these methods have some promise in certain classes of problems, but the cumulative errors introduced by continuous rezoning are poorly understood and these procedures do not overcome the inherent inability of Lagrangian meshes to treat flow around concave corners.

Eulerian fluid meshes, in which the mesh is fixed in space, are well suited to the treatment of large flows and flows around corners. Since the mesh is fixed in space, there is no possibility of mesh distortion. However, when the motions of the structure are large, interfacing between the structural and Eulerian mesh becomes quite difficult: the structural interface may pass through the middle of an Eulerian zone, or cut across a corner, or a corner of the structure may fall within the mesh, etc. The treatment of all of these possibilities requires considerable programming, and it is difficult to make the resulting program applicable to completely arbitrary structures. Similar difficulties are presented by free surfaces, and Eulerian codes often make severe restrictions on their allowed shapes.

In a Quasi-Eulerian treatment of the fluid, the mesh is allowed to move independent of the material. We have used the term Quasi-Eulerian rather than Arbitrary Lagrangian Eulerian (ALE), for the structure of these fluid equations is almost identical to the structure of the Eulerian equations. ALE formulations were developed in a finite difference format by Trulio [1] and Hirt, et al. [2]. These treatments were principally intended for the study of explosive phenomena and the primary motivation for the ALE format was the simplification of the treatment of the boundaries. In the analysis of complex engineering structures by a general purpose program, a finite difference method is not as versatile in treating arbitrary geometries and shapes, so for these purposes a finite element format appears promising.

In this paper, recent developments in the Quasi-Eulerian formulation begun in 1973 [3] and described in [4], [5], [6] are described. A unique feature of this treatment has been the development of a simple amplification matrix scheme for upwinding and some simple schemes for generating the logic for moving the mesh nodes. Other improvements have been the extension of the method to axisymmetric problems, the refinement of certain aspects of the flow around corners and the automatic programming of mesh data. These improvements have been incorporated in the program STRAW and will be briefly described in the following; then some some sample calculations showing the capabilities of the method will be presented.

## 2. Formulation and Equations

Let us denote the spatial (Eulerian) coordinates by $x_i$ and the material (Lagrangian) coordinates by $X_i$. We now introduce mesh coordinates $\xi_i$. If

$$\xi_i = x_i \tag{1}$$

we have an Eulerian mesh, while

$$\xi_i = X_i \tag{2}$$

gives a Lagrangian mesh. If $\xi_i$ is specified independently we have a pseudo-Eulerian mesh. The material velocities are denoted by $v_i$, so

$$v_i = \dot{X}_i \tag{3}$$

where a superscript dot denotes a time derivative. The mesh (grid) velocities are

$$v_i^G = \dot{\xi}_i \tag{4}$$

The motion of the fluid is governed by the equation of motion

$$M_{KL} \dot{v}_{iL} = F_{iK}^{ext} - F_{iK}^{int} \tag{5}$$

where repeated indices indicate summations,

$M_{KL}$ = mass matrix, which is lumped and diagonal

$v_{iL}$ = material velocities at the nodes; lower case indices designate the component number, upper case indices the node number

$F_{iK}^{ext}$ = external nodal forces

$F_{iK}^{int}$ = internal nodal forces

The internal node forces are given by

$$F_{iK}^{int} = \sum_e L_{KJ}^{(e)} \left( f_{iJ}^{int(e)} + t_{iJ}^{(e)} \right) \tag{6}$$

$$f_{iJ}^{int(e)} = \int_{V^{(e)}} p \frac{\partial \dot{J}}{\partial v_{iJ}} \, dV \tag{7}$$

$$t_{iI}^{(e)} = (1 + \gamma_I) \int_{V^{(e)}} \rho N_I \frac{\partial v_i}{\partial x_j} (v_j - v_j^G) \, dV \tag{8}$$

$$\gamma_I = \frac{\overline{UP}}{\gamma} \int_{V^{(e)}} \frac{\partial N_I}{\partial x_i} (v_i - v_i^G) \, dV \tag{9}$$

where $L_{KJ}^{(e)}$ is a Boolean connectivity matrix, $f_{iJ}^{int(e)}$ are the element nodal internal forces, $t_{iI}^{(e)}$ the element nodal transport matrices, $V^{(e)}$ the volume of element e, p the pressure, $\rho$ the density, and $N_I$ the shape functions.

Eq. (5) represents the summation of element nodal forces to the system internal nodal force matrix; Eq. (6) gives the element nodal forces due to the pressure, and Eqs. (7) and (8) give the transport terms. Upwinding is effected through the amplification factors $\gamma_I$, in Eq. (8); $\overline{UP} = 1$ corresponds to full upwinding, $\overline{UP} = 0$ to no upwinding. The factor $\gamma$ is chosen so that $|\gamma_I| \leq 1$ for all I.

The pressure is evaluated by an equation of state

$$p = p(\rho, e) \tag{10}$$

where e is the internal energy. To obtain the density and energy, the continuity and energy balance equations are used. Since the mass of an element does not remain constant in time, $M_{KL}$ must be updated at every time step. The details of these procedures have been reported by Belytschko and Kennedy [5].

The equations of motion are integrated by the explicit central difference method. To evaluate the transport terms, a velocity extrapolation is made; again details are given in [5].

## 3. Automatic Mesh

An inherent drawback of a quasi-Eulerian formulation is that it requires that the motion of the nodes be programmed for the calculation. In the Lagrangian and Eulerian meshes, this is not necessary, for the positions of the mesh points are determined by either Eq. (1) or Eq. (2). This task can easily get out of hand, for in complex configurations, the number of possibilities is extensive. Therefore, an important ingredient of a quasi-Eulerian program is the availability of simple, automatic features for generating the mesh coordinates $x_i$ as a function of time.

One of the schemes we have developed is integrated with the data required for the generation of the initial finite element mesh. The initial nodal data generator uses the simple scheme that all nodes for which nodal data cards are skipped are equispaced between the specified nodes or spaced according to some formula, such as a geometric elongation of successive element sides.

For purposes of generating the mesh coordinates as a function of time, these nodes are flagged initially and either one or both components of the nodes can be designated as Lagrangian. During the computation, the quasi-Eulerian mesh points are then generated by the same formula used initially.

Thus the node cards:

| | | | |
|---|---|---|---|
| 1 | LE | 0.0 | 0.0 |
| 10 | LE | 10.0 | 0.0 |
| 11 | LE | 0.0 | 1.0 |
| 20 | LE | 8.5 | 1.0 |
| 21 | LE | 0.0 | 2.0 |
| 30 | LE | 8.0 | 2.0 |

initially generate a mesh with nodes equispaced from x = 0 to x = 10. During the computation, the x-components of nodes 1, 10, 11, 20, 21 and 30 are treated as Lagrangian, the y-components as Eulerian. Thus the y-components remain unchanged, whereas the x-components are adjusted so that all the nodes between 1-10, 11-20, 21-30 remain equispaced in the x-direction. If a structural wall is placed at x = 10, the fluid will remain in contact with this wall throughout the computation and the mesh will remain relatively undistorted.

The range of problems to which this scheme is applicable is limited, for if $y = 2.0$ corresponds to a free surface, the Eulerian treatment of the y-components would not be appropriate. Therefore, a hierarchial scheme is now under development which permits a separate updating of x- and y-components. To enhance the versatility of the scheme, the coordinate systems may also be rotated locally.

## 4. Results

The first analysis reported here pertains to an SRI experiment [7] which is depicted in Fig. 1. A slow charge was detonated in the center subassembly, and the response of the system was experimentally determined by the strain gauges and pressure transducers shown in Fig. 1. The interiors of the hexcans were empty, but a lightweight transformer oil was used to fill the channels between the hexcans.

The finite element model is shown in Fig. 2; one twelfth symmetry was used. The subassembly walls were modeled by beam elements [8] in a state of plane strain; the material is annealed 316 stainless steel. The plug was 6061-T6 aluminum, and was modeled by triangular finite elements. The fluid was treated as inviscid with a tension cutoff. All material constants are given in Table 1. Slidelines were used between the fluid and beam elements. The fluid nodes were treated as Lagrangian normal to the structure, Eulerian tangential to the structure.

A computer analysis of this problem with the same model was previously reported in [5] for the first 0.8 milliseconds; the computer simulation failed at that point due to difficulties in the treatment of the corner, which caused an instability. This simulation was carried out with no difficulty for 1.2 milliseconds, but it did get rather expensive, requiring 12,000 time steps and 15 CPU minutes on an IBM 370/195.

The pressure in the channel is compared to the experimental results in Figs. 3 and 4. Also shown for comparison is the pressure applied to the inside of the center hexcan. This pressure history for the source is taken from a single hexcan test. [7] suggests a different pressure for the source, with a 14 MPa peak, which we feel is in error. The analysis and experiment agree quite well, particularly if the reduction between applied and channel pressures is considered. The major discrepancies are (1) the absence of the early spikes in the numerical results and (2) the more rapid drop in the pressures at point P2.

Strains at points S1 and S2 are compared with the experiment in Fig. 5. The agreement for both strain gauges is excellent until 0.8 milliseconds; beyond this time, the experiment shows significantly higher strains than the analysis. It is of interest to note that the analysis predicts lower pressures than found experimentally, so the underprediction of the strains is not unexpected. The cause of these trends is not clear, although the pressure input uncertainty may be a factor.

The second example is an SRI pipe experiment [9]. This problem was analyzed with an axisymmetric shell element [10] and axisymmetric quasi-Eulerian elements for the fluid. The material constants are given in Table 2. The nodes in the fluid were treated as Eulerian along the axis of the pipe, Lagrangian normal to it.

The pressure-time histories are compared to experimental results at transducers P4 and P10 (see Fig. 6) in Fig. 7; the comparison is excellent. Strain histories at points A and D (see Fig. 6) are shown in Figs. 8 and 9. In both figures, the five experimental records at each of the cross-section are shown. As can be seen, there is substantial differences be-

cause of the lack of axisymmetry in the experiment. The computation falls nicely near the average value.

Acknowledgment

This work was performed in the Engineering Mechanics Section of the Reactor Analysis and Safety Division at Argonne National Laboratory, under the auspices of the U. S. Department of Energy.

References

[1] TRULIO, J. G., "Theory and Structure of the AFTON Codes," Air Force Weapons Laboratory, AFWL-TR-66-19 (June, 1966).

[2] HIRT, C. W., AMSDEN, A. A., COOK, J. L., "An Arbitrary Lagrangian-Eulerian Computing Method for all Flow Speeds," J. Computational Phys., 14, pp. 227-253 (1974).

[3] BELYTSCHKO, T., KENNEDY, J. M., MARCHERTAS, A. H., "Nonlinear Dynamic Response of Fast-Reactor Core Subassemblies Under Impulsive Loading," Paper E 4/5, Second International Conference on Structural Mechanics in Reactor Technology, Berlin (September, 1973).

[4] KENNEDY, J. M., BELYTSCHKO, T., "Theory and Application of a Quasi-Eulerian Fluid Element for the STRAW Code," ANL-78-100 (October, 1978).

[5] BELYTSCHKO, T., KENNEDY, J. M., "Computer Models for Subassembly Simulation," Nuclear Engineering and Design, 49, pp. 17-38 (1978).

[6] BELYTSCHKO, T., KENNEDY, J. M., SCHOEBERLE, D. F., "Quasi-Eulerian Finite Element Formulation for Fluid-Structural Interaction," Paper 78-PVP-60, ASME/CSME Pressure Vessels & Piping Conference, Montreal, Canada (June, 1978); accepted for publication in Journal of Pressure Vessel Technology.

[7] ROMANDER, C. M., CAGLIOSTRO, D. J., "Experiments on the Response of Hexagon Subassembly Duct Clusters to Central Radial Loads," SRI Report (December, 1976).

[8] BELYTSCHKO, T., HSIEH, B. J., "Nonlinear-Transient Finite Element Analysis with Convected Coordinates," Int. J. Num. Meth. Eng., 7, pp. 255-271 (1973).

[9] ROMANDER, C. M., CAGLIOSTRO, D. J., "Experiments on the Response of Flexible Piping Systems to Internal Pressure Pulses," SRI Report (April, 1976).

[10] BELYTSCHKO, T., HSIEH, B. J., "Nonlinear-Transient Analysis of Shells and Solids of Revolution by Convected Elements," Proc. AIAA/ASME/SAE 14th Struct., Struct. Dyn. and Materials Conf., Williamsburg, Virginia (March, 1973); J. AIAA, 12, pp. 1031-1035 (1974).

Fig. 1. Schematic of SRI Subassembly Experiments; S1 and S2 are Strain Gauges; P1 and P2 are Pressure Transducers.

Fig. 2. Finite Element Model for SRI Experiment.

Fig. 3. Comparison of Computed Pressure (STRAW) with Transducer P1 Record.

Fig. 4. Comparison of Computed Pressure (STRAW) with Transducer P2 Record.

Fig. 5. Comparison of Computed Strains (STRAW) with Strain Gauges S1 and S2.

Fig. 6. Schematic of SRI Pipe Experiment.

Fig. 7. Comparison of Computed Pressures (STRAW) with Experimental Records at P4 and P7.

Fig. 8. Comparison of Computed Hoop Strain (STRAW) with Experimental Records SG1 thru SG5.

Fig. 9. Comparison of Computed Hoop Strain (STRAW) with Experimental Records SG1 thru SG2.

Table I. Subassembly Cluster Test Material Properties

Annealed 316 stainless steel

Young's modulus = $2.122 \times 10^5$ MPa
Poisson's ratio = 0.3
Density = 7850 kg/m$^3$

Uniaxial stress-strain data

| Strain (m/m) | Stress (MPa) |
|---|---|
| 0.000915 | 194.2 |
| 0.002 | 225.1 |
| 0.039 | 362.1 |
| 0.070 | 446.2 |
| 0.170 | 627.5 |
| 0.730 | 1237.8 |
| 2.320 | 1490.5 |

6061T-6 aluminum

Young's modulus = $0.814 \times 10^5$ MPa
Poisson's ratio = 0.3
Density = 2540 kg/m$^3$

Uniaxial stress-strain data

| Strain (m/m) | Stress (MPa) |
|---|---|
| 0.00348 | 283.2 |
| 0.00465 | 326.9 |
| 0.009 | 407.4 |
| 0.100 | 697.3 |

Lightweight transformer fluid

Bulk modulus = $1.67 \times 10^3$ MPa
Density = 850 kg/m$^3$

Table II. Pipe Test Material Properties

Nickel 200

Young's modulus = $1.93 \times 10^5$ MPa
Poisson's ratio = 0.3
Density = 8850 kg/m$^3$

Uniaxial stress-strain data

| Strain (m/m) | Stress (MPa) |
|---|---|
| 0.000393 | 76.0 |
| 0.00127 | 95.0 |
| 0.0058 | 118.6 |
| 0.1 | 384.0 |

Water

Bulk modulus = $2.07 \times 10^3$ MPa
Density = 1000 kg/m$^3$

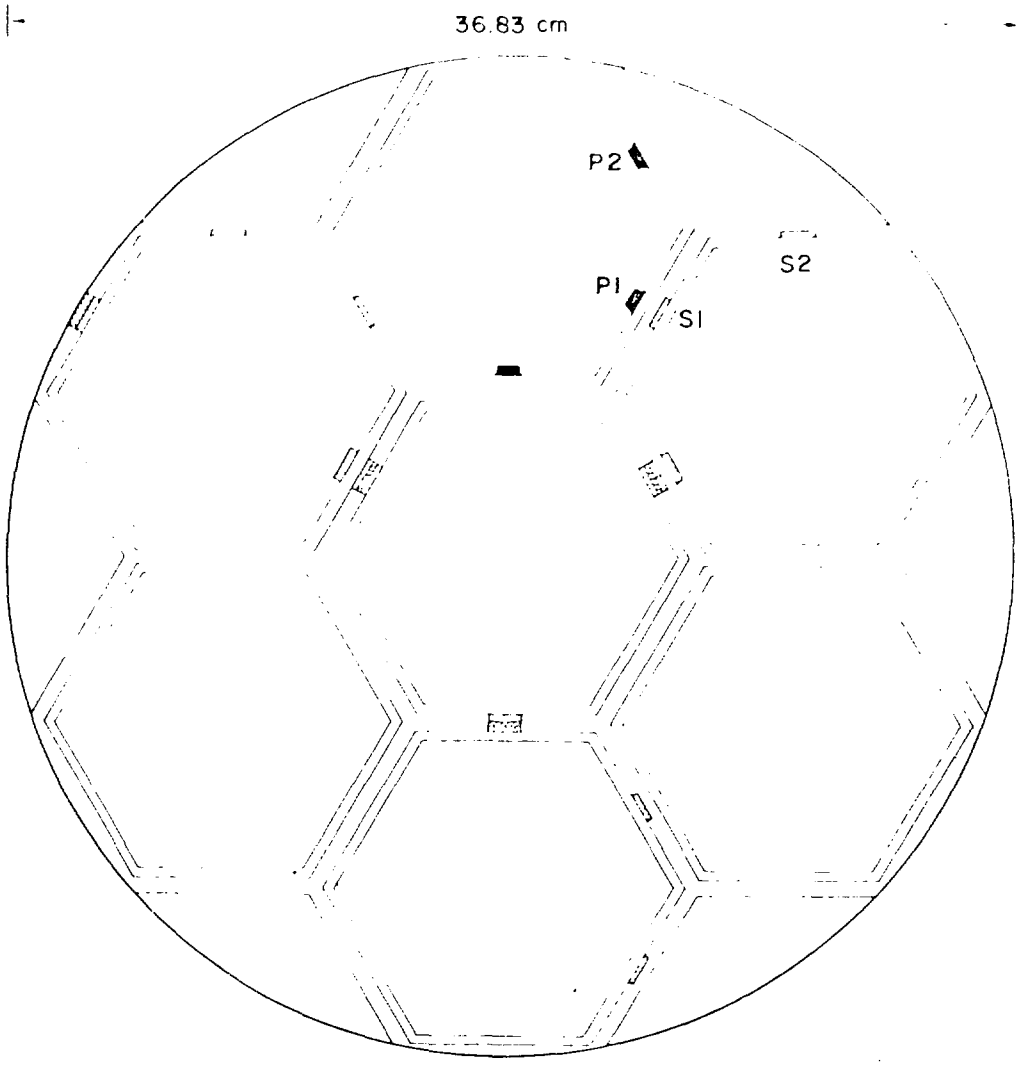
36.83 cm
P2
S2
P1
S1

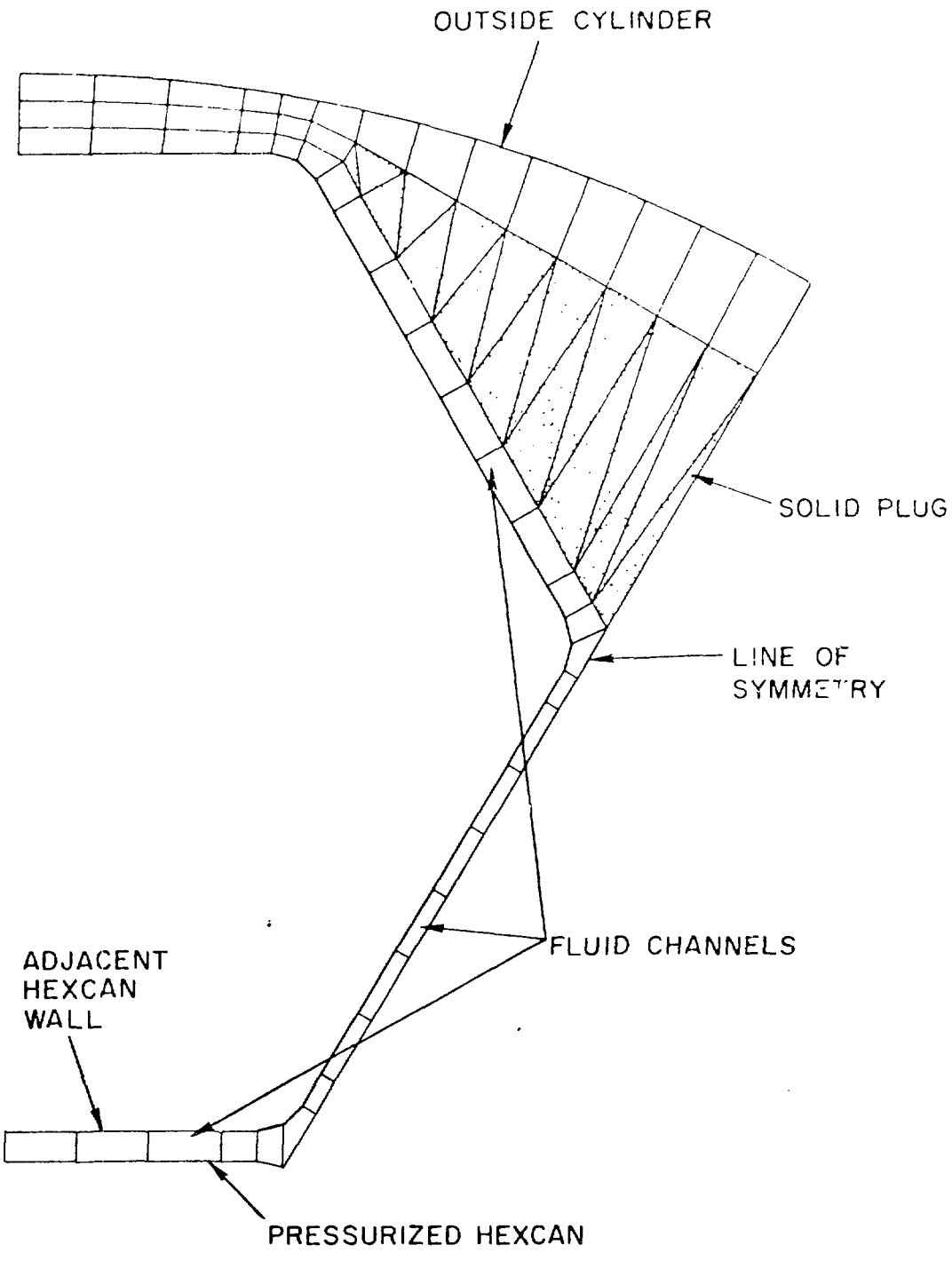
OUTSIDE CYLINDER
SOLID PLUG
LINE OF
SYMMETRY
FLUID CHANNELS
ADJACENT
HEXCAN
WALL
PRESSURIZED HEXCAN

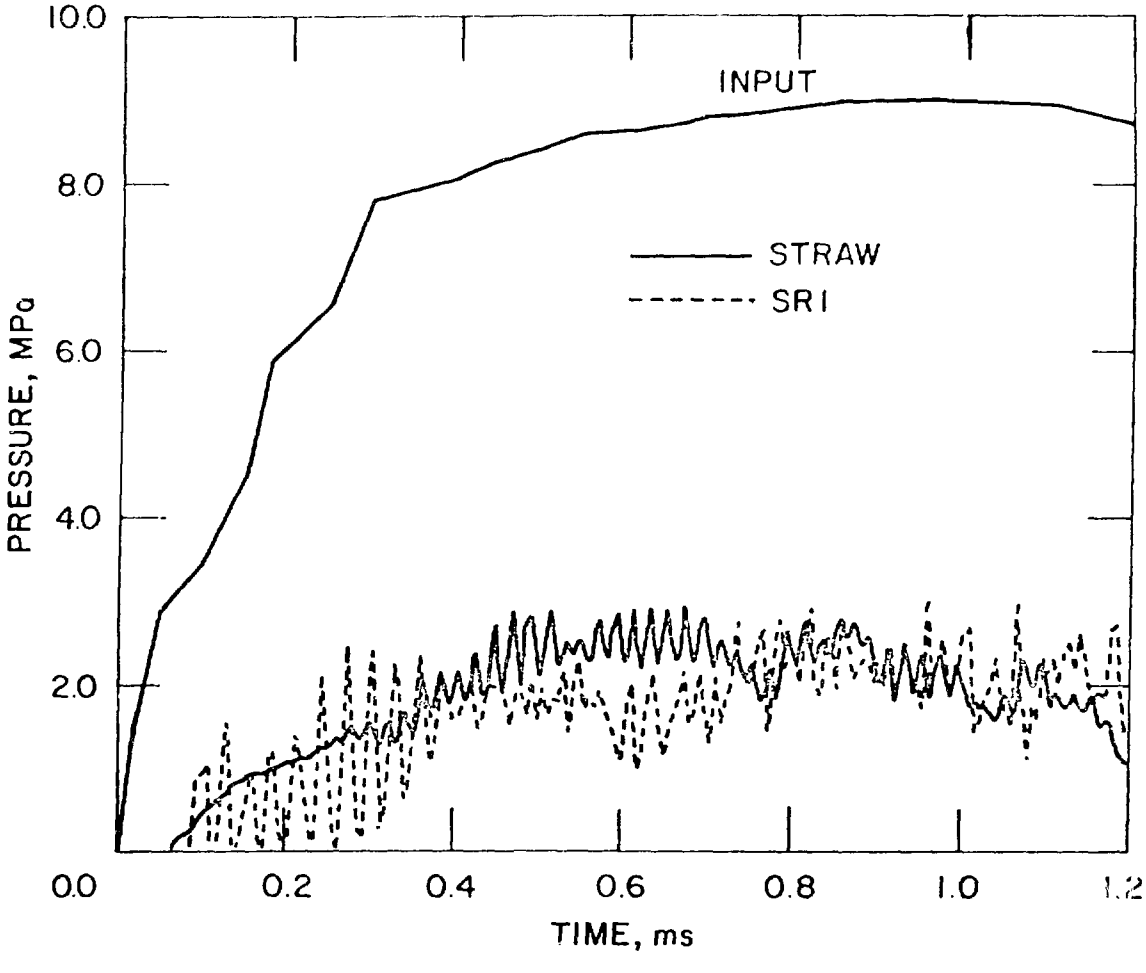
10.0
8.0
6.0
4.0
2.0
0.0
PRESSURE, MPa
INPUT
STRAW
SR1
0.2
0.4
0.6
0.8
1.0
1.2
TIME, ms

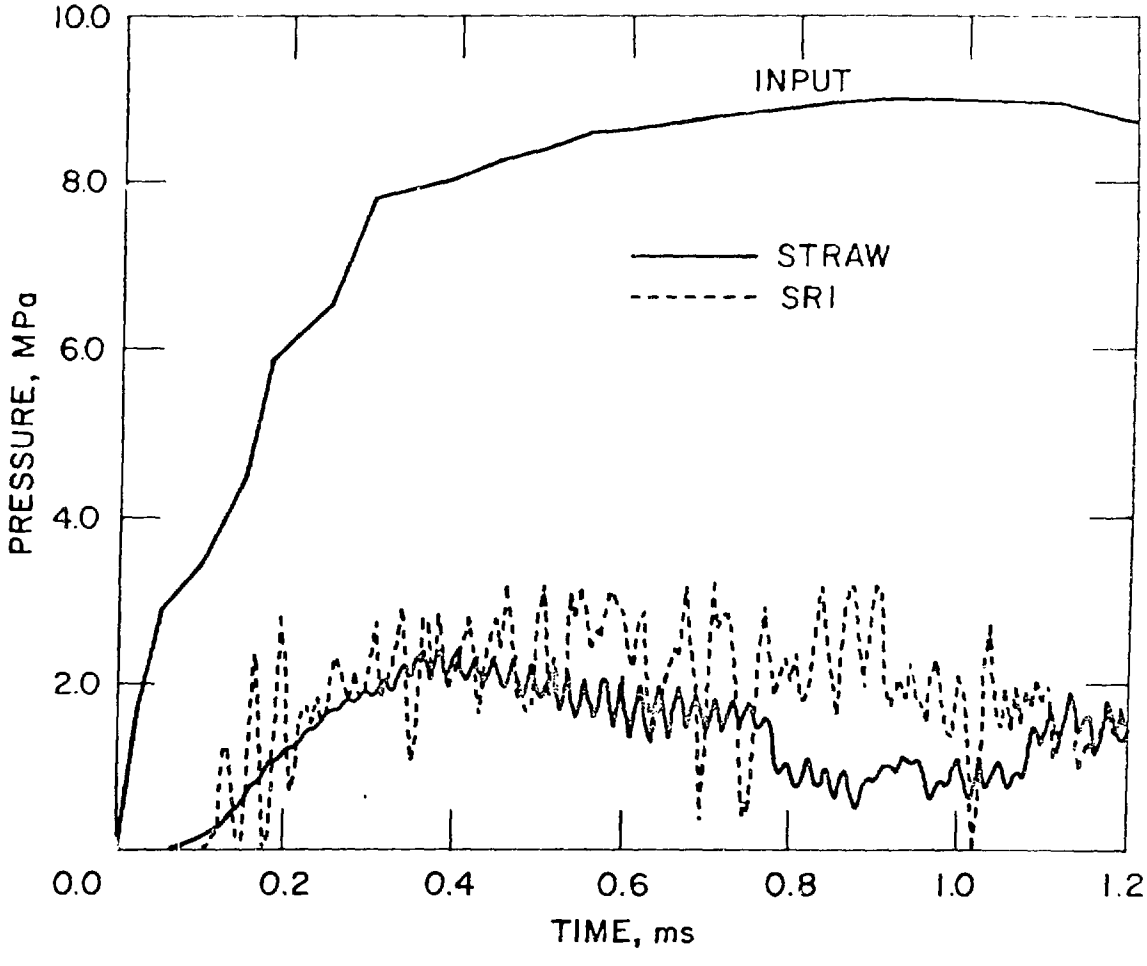
10.0
8.0
6.0
4.0
2.0
0.0
PRESSURE, MPa
INPUT
STRAW
SRI
0.2
0.4
0.6
0.8
1.0
1.2
TIME, ms

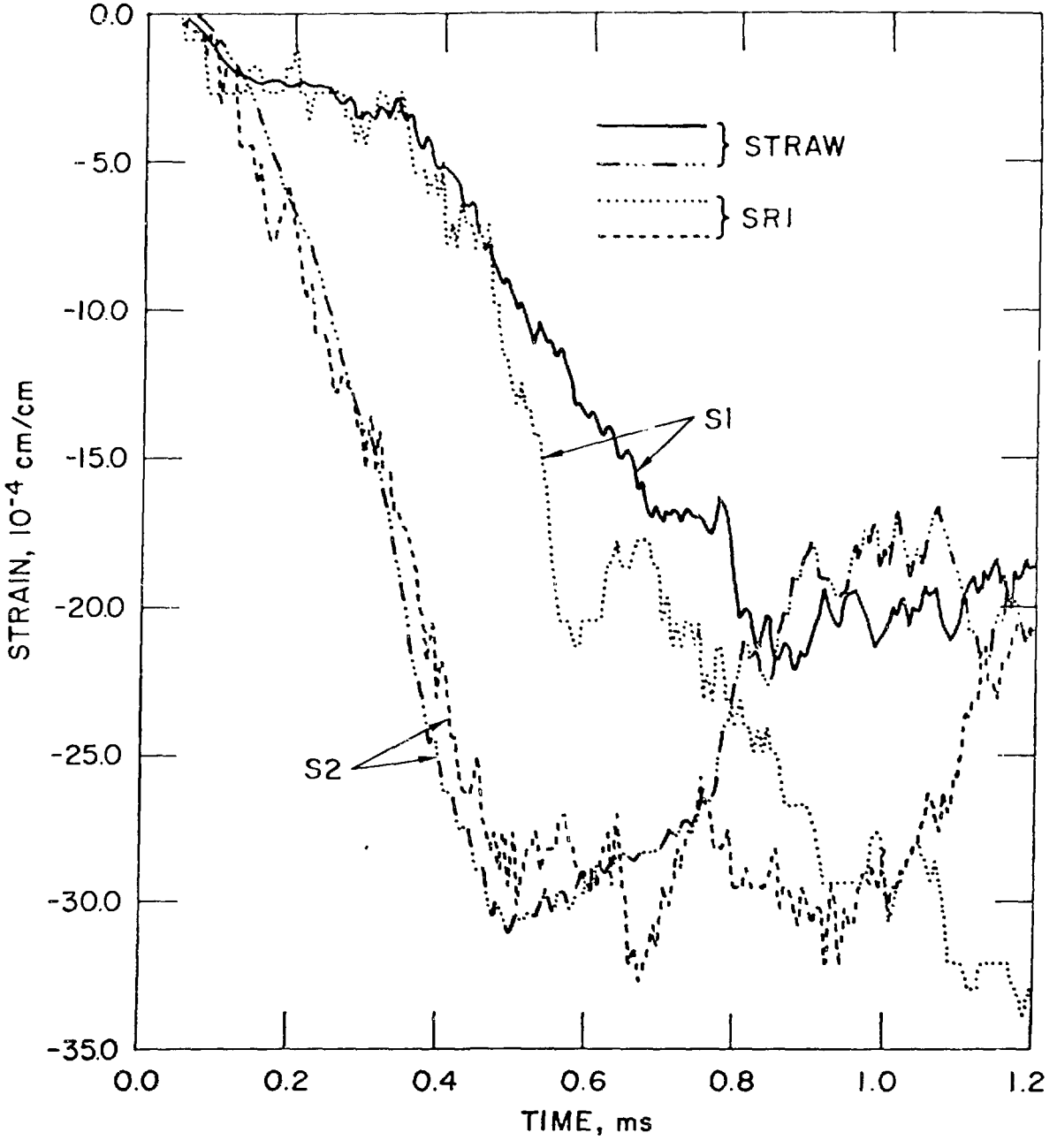
0.0
-5.0
-10.0
-15.0
-20.0
-25.0
-30.0
-35.0
STRAIN, $10^{-4}$ cm/cm
0.0
0.2
0.4
0.6
0.8
1.0
1.2
TIME, ms
STRAW
SRI
S1
S2

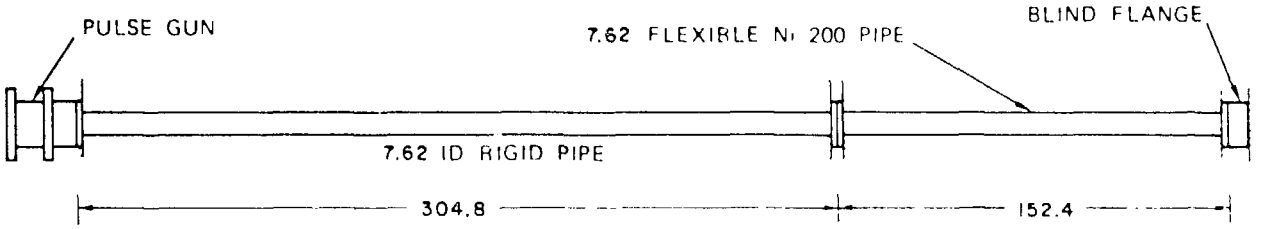


(a) STRAIGHT-PIPE TEST CONFIGURATION

ALL DIMENSIONS IN cm

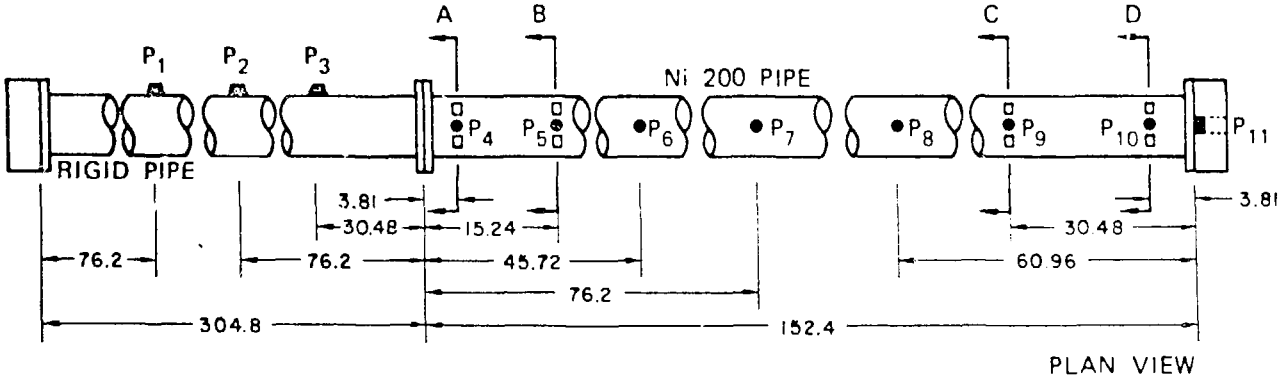


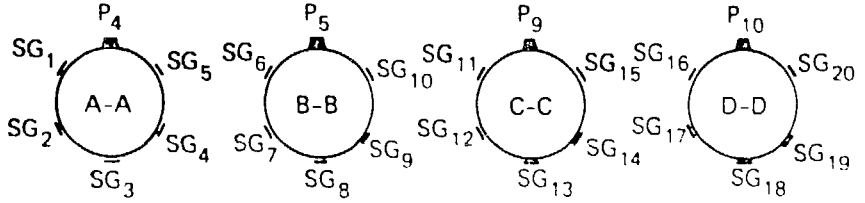


(b) INSTRUMENTATION FOR STRAIGHT-PIPE TEST

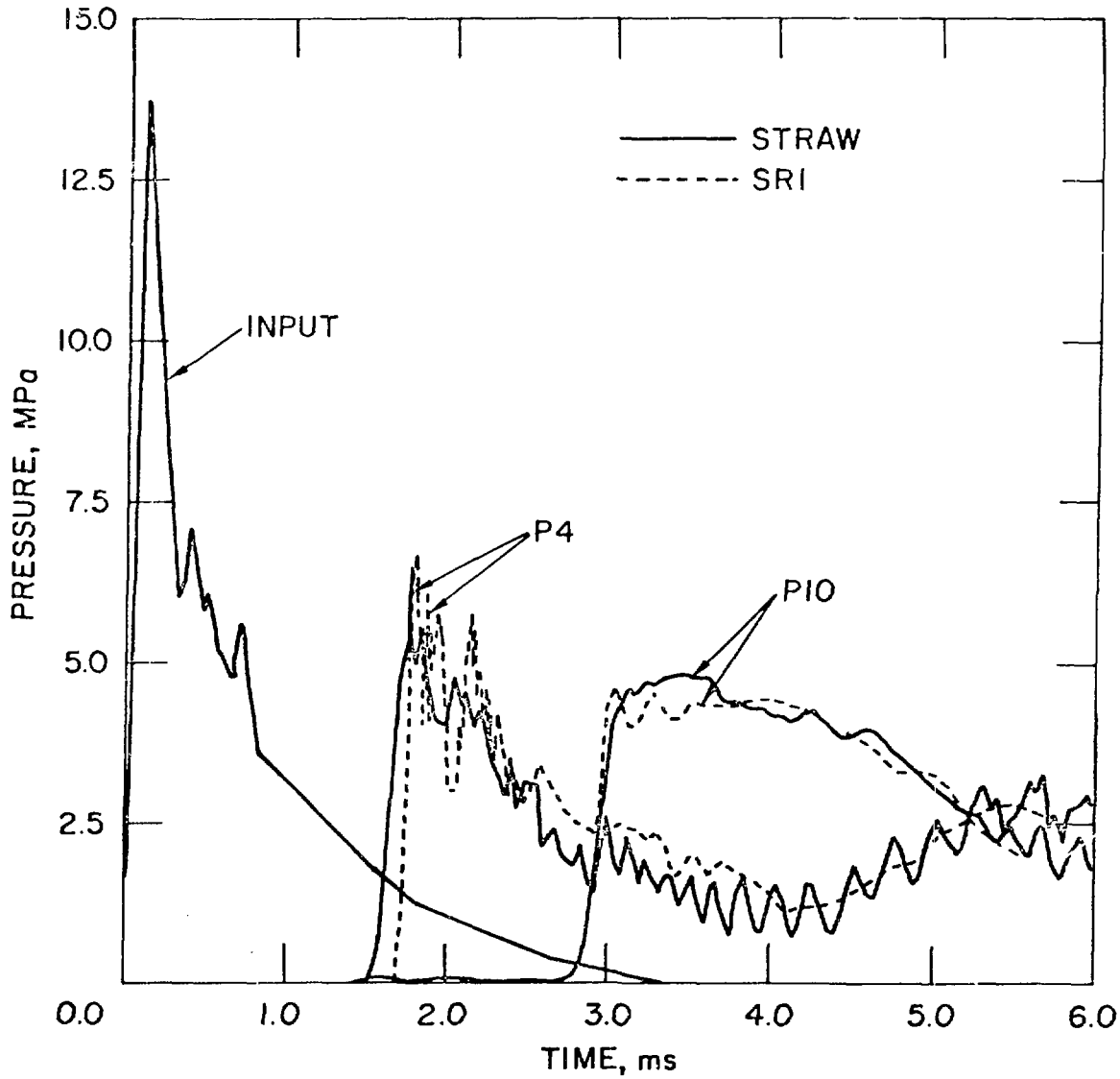
15.0
12.5
10.0
7.5
5.0
2.5
0.0
1.0
2.0
3.0
4.0
5.0
6.0
PRESSURE, MPa
TIME, ms
STRAW
SRI
INPUT
P4
P10

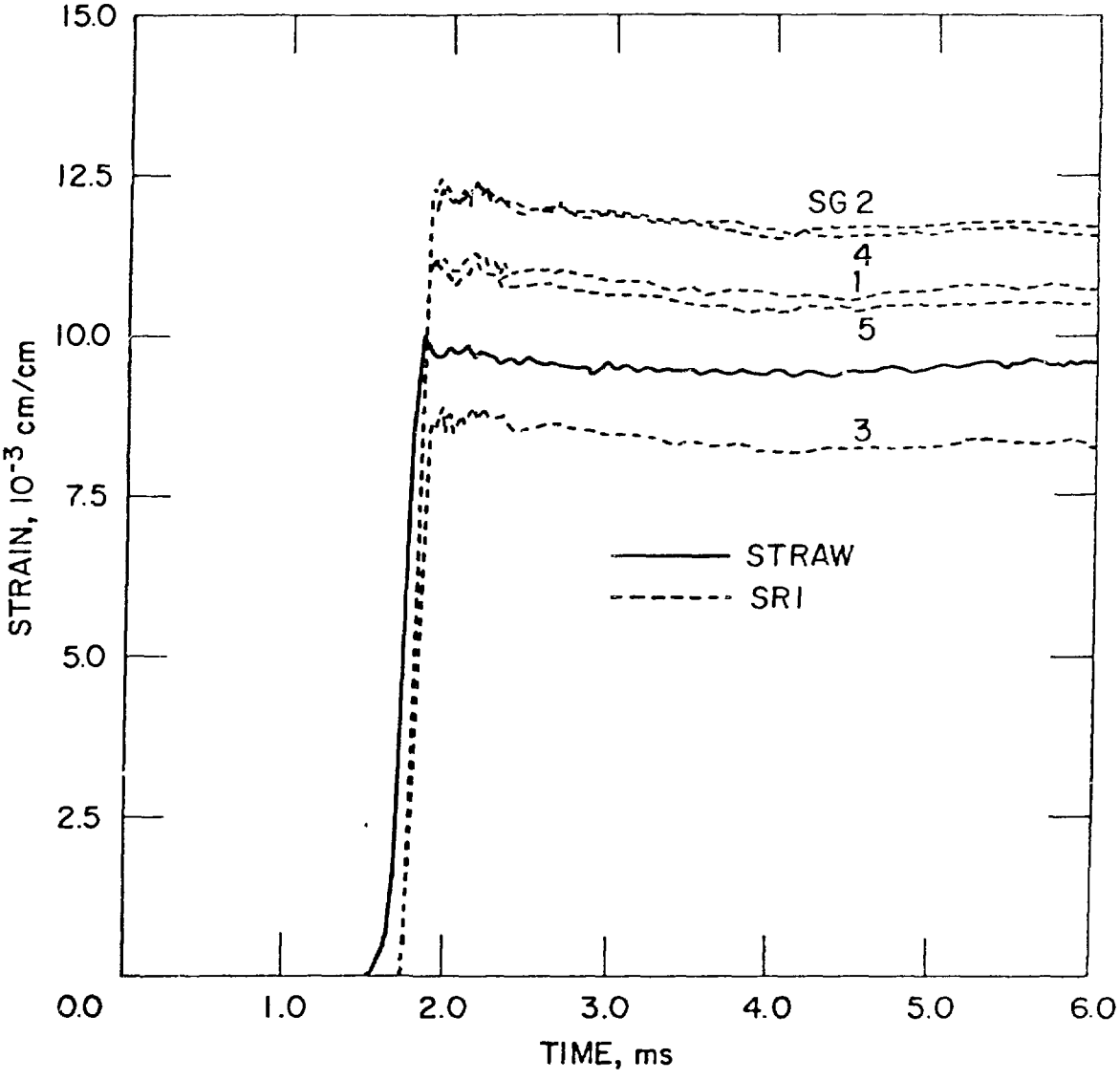
15.0
12.5
10.0
7.5
5.0
2.5
0.0
STRAIN, $10^{-3}$ cm/cm
1.0
2.0
3.0
4.0
5.0
6.0
TIME, ms
SG 2
4
1
5
3
STRAW
SRI

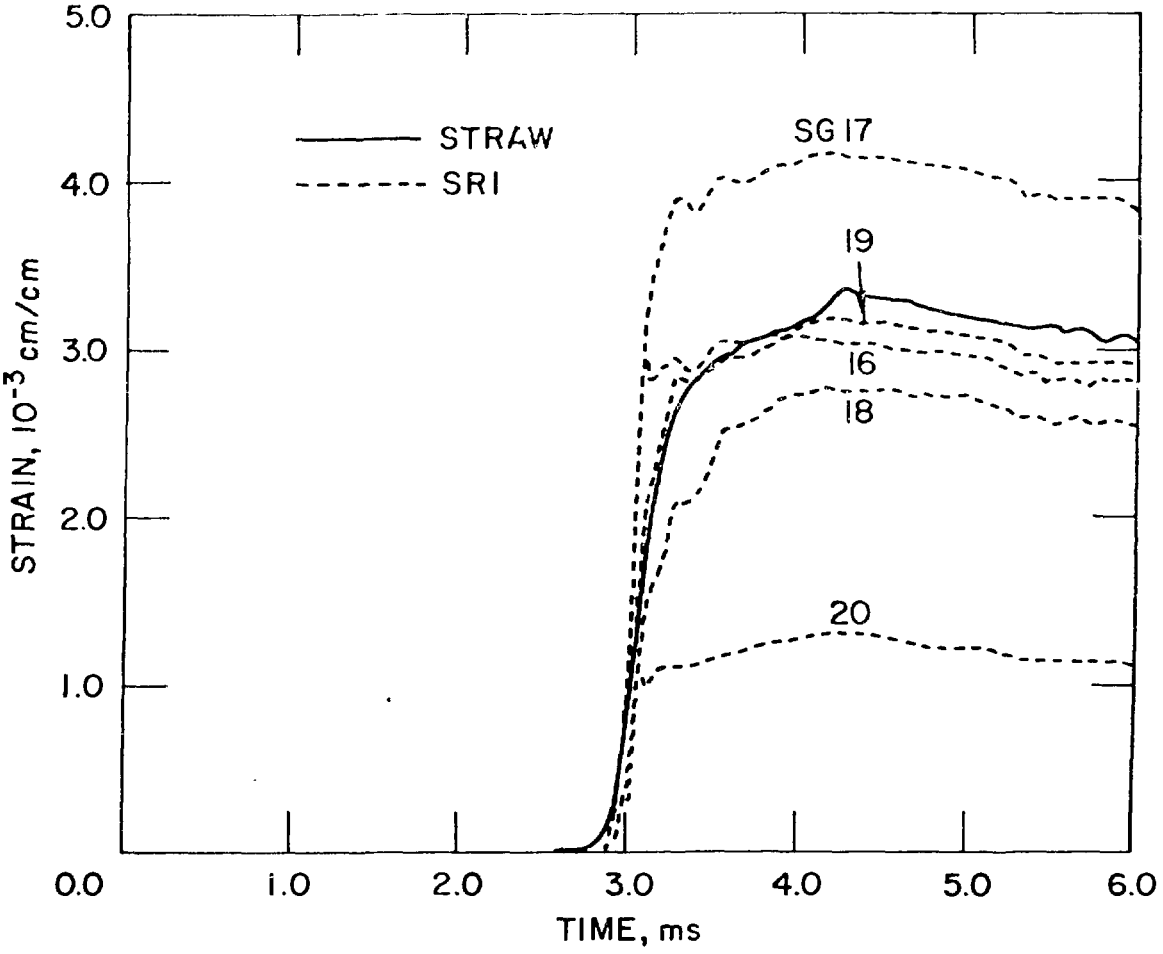
5.0
4.0
3.0
2.0
1.0
0.0
STRAIN, $10^{-3}$ cm/cm
STRAW
SRI
SG 17
19
16
18
20
1.0
2.0
3.0
4.0
5.0
6.0
TIME, ms